

# MobileNetV4 - Universal Models for the Mobile Ecosystem

Danfeng Qin<sup>†‡</sup>, Chas Leichner<sup>†‡</sup>, Manolis Delakis<sup>†</sup>, Marco Fornoni, Shixin Luo, Fan Yang, Weijun Wang, Colby Banbury, Chengxi Ye, Berkin Akin, Vaibhav Aggarwal, Tenghui Zhu, Daniele Moro, and Andrew Howard<sup>†§</sup>

Google

**Abstract.** We present the latest generation of MobileNets, known as MobileNetV4 (MNv4), featuring universally efficient architecture designs for mobile devices. At its core, we introduce the Universal Inverted Bottleneck (UIB) search block, a unified and flexible structure that merges Inverted Bottleneck (IB), ConvNext, Feed Forward Network (FFN), and a novel Extra Depthwise (ExtraDW) variant. Alongside UIB, we present Mobile MQA, an attention block tailored for mobile accelerators, delivering a significant 39% speedup. An optimized neural architecture search (NAS) recipe is also introduced which improves MNv4 search effectiveness. The integration of UIB, Mobile MQA and the refined NAS recipe results in a new suite of MNv4 models that are mostly Pareto optimal across mobile CPUs, DSPs, GPUs, as well as specialized accelerators like Apple Neural Engine and Google Pixel EdgeTPU - a characteristic not found in any other models tested. Finally, to further boost accuracy, we introduce a novel distillation technique. Enhanced by this technique, our MNv4-Hybrid-Large model delivers 87% ImageNet-1K accuracy, with a Pixel 8 EdgeTPU runtime of just 3.8ms.<sup>1</sup>

## 1 Introduction

Efficient on-device neural networks not only enable fast, real-time and interactive experiences, but also avoid streaming private data through the public internet. However, the computational constraints of mobile devices pose the significant challenge of balancing accuracy and efficiency. To this end, we introduce UIB and Mobile MQA, two innovative building blocks, integrated via a refined NAS recipe to create a series of universally mostly-Pareto-optimal mobile models. Additionally, we present a distillation technique that further improves accuracy.

Our Universal Inverted Bottleneck (UIB) block improves the Inverted Bottleneck block [36] by incorporating two optional depthwise convolutions [19]. Despite its simplicity, UIB unifies prominent micro-architectures - Inverse Bottleneck (IB), ConvNext [32], and FFN [12] - and introduces the Extra Depthwise

<sup>0</sup> †Equal primary contribution. ‡Project Lead. §Senior Lead.

<sup>1</sup> All MobileNetV4 models are available at <https://github.com/tensorflow/models/blob/master/official/vision/modeling/backbones/mobilenet.py>

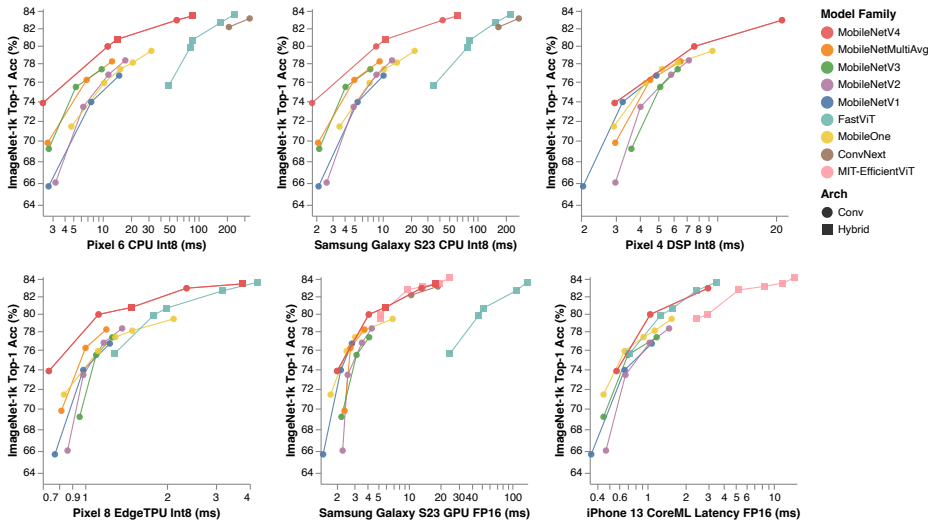


**Fig. 1: MNv4 Models are Universally Mostly Pareto Optimal:** MNv4 performs strongly compared to leading efficient models across diverse hardware. All models were trained on ImageNet-1k solely. Most models were optimized for one device, but MNv4 is Pareto optimal across most devices. Hybrid models and ConvNext are DSP-incompatible. Due to PyTorch-to-TFLite export tool limitations, EfficientViTs [13] [14] are not benchmarked on CPUs and EdgeTPU. MNv4-Hybrid models were excluded from CoreML evaluation due to the lack of PyTorch implementation of Mobile MQA.

(ExtraDW) IB block. UIB offers flexibility in spatial and channel mixing, the option to extend the receptive field, and enhanced computational efficiency.

Our optimized Mobile MQA block achieves over a 39% inference speedup on mobile accelerators with respect to Multi-Head Attention [44].

Our two-phase NAS approach, separating coarse and fine-grained searches, significantly boosts search efficiency and facilitates the creation of models that are significantly larger than previous state-of-the-art models [41]. Additionally, incorporating an offline distillation dataset reduces noise in NAS reward measurements, resulting in improved model quality.

By integrating UIB, MQA, and the improved NAS recipe, we present the MNv4 suite of models, achieving mostly Pareto optimal performance across diverse hardware platforms, including CPUs, DSPs, GPUs, and specialized accelerators. Our model series encompasses a computational spectrum ranging from the extremely compact MNv4-Conv-S design, with 3.8M parameters and 0.2G MACs, achieving 73.8% top-1 ImageNet-1K accuracy within 2.4 ms on the Pixel 6 CPU, to the MNv4-Hybrid-L high-end variant that establishes a new reference for mobile model accuracy, operating at 3.8 ms on the Pixel 8 EdgeTPU. Our novel distillation recipe mixes datasets with different augmentations and adds balanced in-class data, enhancing generalization and further increasing accuracy. With this technique, MNv4-Hybrid-L achieves an impressive 87% top-1 accuracy on ImageNet-1K: a mere 0.5% drop compared to its teacher, despite having 39x less MACs.

## 2 Related Work

Optimizing models for both accuracy and efficiency is a well studied problem.

**Mobile Convolutional Networks:** Key work includes MobileNetV1 [20] with depthwise-separable convolutions for better efficiency, MobileNetV2 [36] introducing linear bottlenecks and inverted residuals, MnasNet [40] integrating lightweight attention in bottlenecks, and MobileOne [43] adding and re-parameterizing linear branches in inverted bottlenecks at inference time.

**Efficient Hybrid Networks:** This line of research integrates convolutional and attention mechanisms. MobileViT [33] merges CNN strengths with ViT [12] through global attention blocks. MobileFormer [6] parallelizes a MobileNet and a Transformer with a two-way bridge in between for feature fusing. FastViT [42] adds attention to the last stage and uses large convolutional kernels as a substitute for self-attention in the early stages.

**Efficient Attention:** Research has focused on enhancing MHSA [44] efficiency. EfficientViT [13] and MobileViTv2 [34] introduce self-attention approximations for linear complexity with minor accuracy impacts. EfficientFormerV2 [27] downsamples Q, K, V for efficiency, while CMT [15] and NextViT [26] downsample only K and V.

**Hardware-aware Neural Architecture Search (NAS):** Another common technique is to automate the model design process using hardware-aware Neural Architecture Search (NAS). NetAdapt [49] uses empirical latency tables to optimize the accuracy of a model under a target latency constraint. MnasNet [40] also uses latency tables, but applies reinforcement learning to do hardware-aware NAS. FBNet [47] accelerates multi-task hardware-aware search via differentiable NAS. MobileNetV3 [18] is tuned to mobile phone CPUs through a combination of hardware-aware NAS, the NetAdapt algorithm, and architecture advances. MobileNet MultiHardware [8] optimizes a single model for multiple hardware targets. Once-for-all [5] separates training and search for efficiency.

## 3 Hardware-Independent Pareto Efficiency

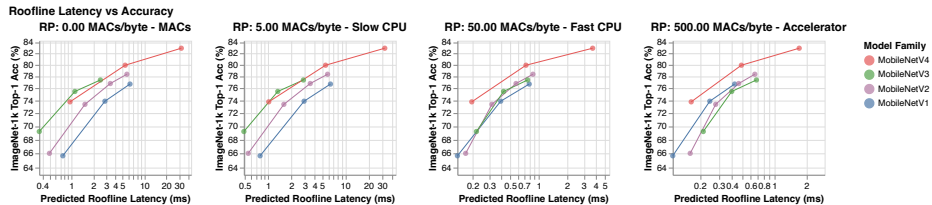


**Fig. 2: Ridge Points and Latency/Accuracy Trade-Offs:** The ridge point measures the relationship between memory bandwidth MACs relate in the roofline performance model. If memory bandwidth is constant, high-compute hardware (accelerators) have a higher ridge point than low-compute hardware (CPUs). MobileNetV4 is mostly Pareto-optimal from a ridge point of 0 to 500 MACs/byte. These analytically-derived (Eqs. 1) charts reflect the real hardware measurements in Figure 1.

**The Roofline Model:** For a model to be universally efficient, it must per-

form well on hardware targets with vastly different bottlenecks that limit the model’s performance. These bottlenecks are largely determined by the hardware’s peak computational throughput and its peak memory bandwidth.

To this end, we use the Roofline Model [46] which estimates the performance of a given workload and predicts whether it is memory-bottlenecked, or compute-bottlenecked. In short, it abstracts away specific hardware details and only considers a workload’s operational intensity ( $\text{LayerMACs}_i / (\text{WeightBytes}_i + \text{ActivationBytes}_i)$ ) vs. the theoretical limits of the hardware’s processor and memory system. Memory and compute operations happen roughly in parallel, so the slower of the two approximately determines the latency bottleneck. To apply the Roofline Model to neural networks with layers indexed by  $i$ , we can calculate the model inference latency,  $\text{ModelTime}$ , as follows:

$$\begin{aligned} \text{ModelTime} &= \sum_i \max(\text{MACTime}_i, \text{MemTime}_i) \\ \text{MACTime}_i &= \frac{\text{LayerMACs}_i}{\text{PeakMACs}}, \quad \text{MemTime}_i = \frac{\text{WeightBytes}_i + \text{ActivationBytes}_i}{\text{PeakMemBW}} \end{aligned} \quad (1)$$

In the roofline model, hardware behavior is summarized by the *Ridge Point* (RP)—the ratio of a hardware’s PeakMACs to PeakMemBW. I.e. the minimum operational intensity required to achieve maximum performance.<sup>2</sup> In order to optimize for hardware with a wide range of bottlenecks, as seen in Fig. 2 and Fig. 3 we analyze our algorithms’ latency while sweeping the RP from its lowest expected value (0 MAC/byte) to its highest expected value (500 MACs/byte)—see Appendix F for more details. Roofline Models only depend on the ratio of data transfer to compute, so all hardware with the same RP will rank workloads the same by latency.<sup>3</sup> This means that swept-RP roofline analysis (see next paragraph) applies to future hardware and software if the RP of the new targets is contained in the swept range.

**Ridge Point Sweep Analysis:** As seen in Fig. 2 and Fig. 3, the roofline model sheds light on how MobileNetV4 models achieve hardware-independent mostly-Pareto-optimal performance against other convolutional MobileNets. On low-RP hardware (e.g. CPUs), models are more likely to be compute-bound than memory-bound. So, to improve latency you minimize the total number of MACs even at the cost of increased memory complexity (MobileNetV3Large-1.5x). Data movement is the bottleneck on high-RP hardware, so MACs do not meaningfully slow down the model but can increase model capacity (MobileNetV1-1.5x). So models optimized for low-RPs run slowly at high-RPs because memory-intensive and low-MAC fully-connected (FC) layers become are bottlenecked on memory bandwidth and can’t take advantage of the high available PeakMACs.

<sup>2</sup> The common practice of using a model’s total MACs to proxy latency is the same as targeting a roofline model with a Ridge Point (RP) = 0. This is equivalent to infinite bytes per MAC so,  $\forall i, \text{MemTime}_i = 0$  and  $\text{ModelTime} = \sum_i \text{MACTime}_i$ .

<sup>3</sup> The Roofline Model assumes that software implementation has no impact on workload performance. This means techniques with complex memory access (e.g. pruning) perform much better on a Roofline Model than on a real device.

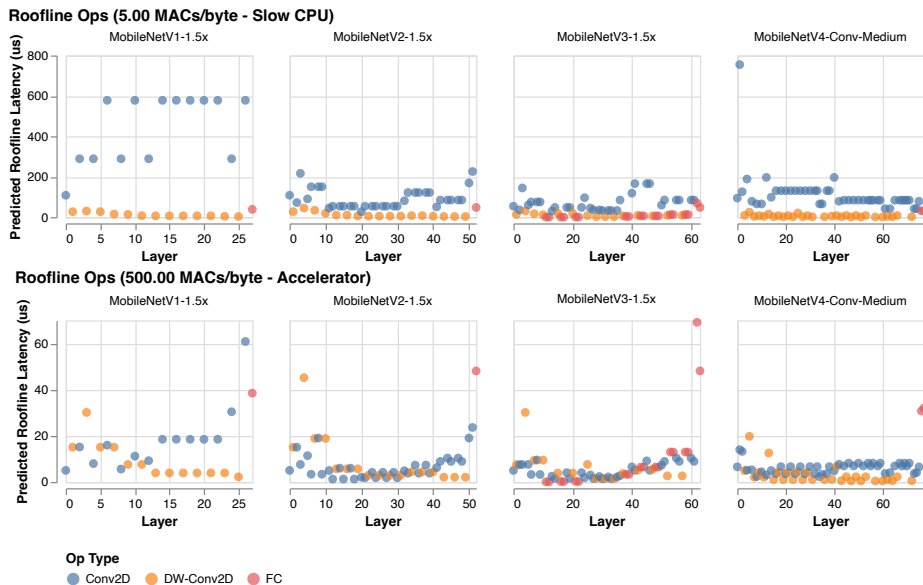


**Fig. 3: Op Cost vs Ridge Point:** Each sub-chart displays the roofline latency (Eqs. 1) of a network’s ops. Networks start on the left. Large Conv2Ds are expensive on low ridge point (RP) hardware (top row), but add cheap model capacity on high-RP hardware (bottom row). FC layers and DW-Conv2Ds are cheap at low RPs and expensive at high RPs. MobileNetV4 balances MAC-intensive Conv2D layers and memory-intensive FC layers where they contribute most to the network—the beginning and end, respectively.

**MobileNetV4 Design:** MobileNetV4 balances investing MACs and memory bandwidth where they will provide the maximum return for the cost, paying particular attention to the start and end of the network. At the beginning of the network, MobileNetV4 uses large and expensive initial layers to substantially improve the models’ capacity and downstream accuracy. These initial layers are dominated by a high number of MACs, so they are only expensive on low-RP hardware. At the end of the network, all MobileNetV4 variants use the same size final FC layers to maximize accuracy, even though this causes smaller MNV4 variants to suffer higher FC latency on high-RP hardware. Since large initial Conv layers are expensive on low-RP hardware, but not high-RP hardware and the final FC layers are expensive on high-RP hardware, but not low-RP hardware, MobileNetV4 models will never see both slowdowns at the same time. In other words, MNv4 models are able to use expensive layers that disproportionately improve accuracy but not suffer the simultaneous combined costs of the layers, resulting in mostly Pareto-optimal performance at all ridge points.

## 4 Universal Inverted Bottlenecks

We present the Universal Inverted Bottleneck (UIB) Block, an adaptable building block for efficient network design that has the flexibility to adapt to a variety of optimization targets without exploding search complexity. UIB extends the

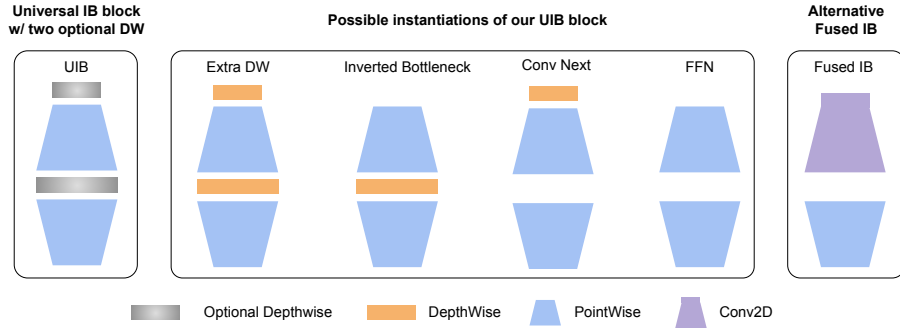


**Fig. 4:** Universal Inverted Bottleneck (UIB) blocks.

inverted bottleneck (IB) block, introduced by MobileNetV2 [36], which has become the standard building block for efficient networks [12, 18, 32, 41].

Building on top of the most successful MobileNet ingredients - separable depthwise convolution (DW) and pointwise (PW) expansion and projection inverted bottleneck structure, this paper introduces a new building block - Universal Inverted Bottleneck (UIB) block, as shown in Figure 4. Its structure is rather simple. We introduce two optional DWs in the Inverted BottleNeck block, one before the expansion layer, and one between the expansion and projection layer. The presence or absence of these DWs is part of the NAS optimization procedure, resulting in novel architectures. Despite the simplicity of this modification, our new building block nicely unifies a few important existing blocks, including the original IB block, ConvNext block, and the FFN block in ViT. Additionally, UIB introduces a new variant: the Extra depthwise IB (ExtraDW) block.

In addition to allowing for a flexible IB structure during NAS, we avoid any human-crafted scaling rule, such as the one used in EfficientNet, and instead individually optimize the structure for each model size. To avoid exploding the size of the NAS SuperNet, we shared the common components (pointwise expansion and projection) and simply added the DWs as extra search options. In combination with the SuperNet based Network Architecture Search algorithm, this approach enables sharing of most of the parameters (>95%) across different instantiations, making NAS extremely efficient.

**UIB Instantiations** The two optional depthwise convolutions in the UIB block have four possible instantiations (Fig. 4), resulting in different tradeoffs.

**Inverted Bottleneck (IB)** - performs spatial mixing on the expanded features activations, providing greater model capacity at increased cost.

**ConvNext** allows for a cheaper spatial mixing with larger kernel size by performing the spatial mixing before the expansion.

**ExtraDW** is a new variant introduced in this paper that allows for an inexpensive increase of the network depth and the receptive field. It offers the

combined benefits of ConvNext and IB.<sup>4</sup>

**FFN** is a stack of two 1x1 pointwise convolutions (PW) with activation and normalization layers in between. PW is one of the most accelerator-friendly operations but works best when used with other blocks.

At each network stage, UIB provides flexibility to (1) Strike an ad-hoc spatial and channel mixing tradeoff. (2) Enlarge the receptive field as needed. (3) Maximize the computational utilization.

## 5 Mobile MQA

In this section, we present Mobile MQA, a novel attention block that is specifically optimized for accelerators, and provides over 39% inference speed up.

**Importance of Operational Intensity:** Recent research in vision models has largely focused on reducing arithmetic operations (MACs) to enhance efficiency. However, the real bottleneck for performance on mobile accelerators is often not computation but memory access. This is because accelerators provide far greater computational power than memory bandwidth. Therefore, simply minimizing MACs may not lead to better performance. Instead, we must consider the Operational Intensity, the ratio of arithmetic operations to memory access.

**MQA is efficient in hybrid models:** MHSA [44] projects the queries, keys, and values into multiple spaces to capture different aspects of the information. Multi-Query Attention (MQA) [37] simplifies this by using shared keys and values across all heads. While multiple query heads are essential, large language models can effectively share a single head for keys and values without sacrificing accuracy [7] [25]. One shared head for keys and values greatly reduce the memory access needs when the number of batched tokens is relatively small compared to the feature dimensions, and thus significantly improves Operational Intensity. This is typically the case for hybrid vision models for mobile applications, where attention is employed only in the low-resolution later stages with high feature dimensions, and batch size is normally one. Our experiments confirm MQA’s advantage in hybrid models. As shown in Table 1, compared to MHSA, MQA achieves over 39% acceleration on EdgeTPUs and Samsung S23 GPU with negligible quality loss (-0.03%). MQA also reduces MACs and model parameters by over 25%. To our knowledge, we are the first to use MQA for mobile vision.

**Incorporate asymmetric spatial down-sampling:** Drawing inspiration from MQA, which utilizes asymmetric computation across queries, keys, and values, we incorporate Spatial Reduction Attention (SRA) [45] to our optimized MQA block to downscale the resolution of keys and values, yet retain high-resolution queries. This strategy is motivated by the observed correlation between spatially adjacent tokens in hybrid models, attributed to spatial mixing convolution filters in early layers. Through asymmetric spatial down-sampling, we maintain the same token count between input and output, preserving attention’s high res-

<sup>4</sup> It could be seen as a MobileNetV1 style factorization of two standard convolutional blocks.

model	Top-1	MACs (G)	Params (M)	EdgeTPU		Samsung S23 GPU
	Acc(%)			Pixel 7	Pixel 8	
base model	84.88	6.0	30.9	4.31 ms	2.35 ms	13.15 ms
+3 MHSA	85.27	6.7	36.0	9.69 ms	2.76 ms	16.46 ms
+3 MQA	85.24 (-0.03%)	6.5 (-28.6%)	34.7 (-25.5%)	5.16 ms (-84.2%)	2.60 ms (-39.0%)	15.10ms (41.1%)

**Table 1: Efficiency Gains by MQA.** Base model is MNv4-Conv-L. Additional attention blocks are added to the last stage. Reported percentage improvements are comparing only the latency of the attention blocks (baseline MHSA).

**Table 2: Improvements via Asymmetric Spatial Downsampling in Mobile MQA:** Used MNv4-Hybrid-M as the base model, evaluated on Samsung S23. Down-sampling with a stride of 2 is applied at the penultimate stage of 16x16 pixels.

down-sampling on KV	Top-1 Acc	MACs (G)	CPU (ms)	GPU (ms)
No	80.77	1.285	15.8	7.4
Yes	80.71	1.245	12.8	5.9
Efficiency Gain	-	+3%	+23%	+25%

olution and significantly enhancing efficiency. Unlike [45], our method replaces AvgPooling with a 3x3 depthwise convolution using a stride of 2 for spatial reduction, offering a cost-effective way to boost model capacity.

**Mobile MQA** Here we present our Mobile MQA block:

$$\text{Mobile\_MQA}(\mathbf{X}) = \text{Concat}(\text{attention}_1, \dots, \text{attention}_n) \mathbf{W}^O$$

$$\text{where } \text{attention}_j = \text{softmax} \left( \frac{(\mathbf{X} \mathbf{W}^{Q_j})(SR(\mathbf{X}) \mathbf{W}^K)^T}{\sqrt{d_k}} \right) (SR(\mathbf{X}) \mathbf{W}^V) \quad (2)$$

where  $SR$  denotes either spatial reduction, a DW with stride of 2 in our design, or the identity function in the case that spacial reduction isn't used. As shown in Table 2, incorporating asymmetric spatial down-sampling yields over 20% efficiency gain with minimal accuracy loss (-0.06%).

## 6 Design of MNv4 Models

**Our Design Philosophy: Simplicity Meets Efficiency.** In developing the latest MobileNets, our core goal was Pareto optimality across diverse mobile platforms. To achieve this, we started by conducting extensive correlation analyses on existing models and hardware. Through empirical examination, we found a set of components and parameters that both ensure high correlations between cost models (the prediction of cost of latency) across various devices and approach the Pareto frontier in performance.

Our investigation unveiled critical insights:

*Multi-path efficiency concerns:* Group convolutions [52] and similar multi-path designs, despite lower FLOP counts, can be less efficient due to memory access complexity.

*Hardware support matters:* Advanced modules like Squeeze and Excite (SE) [21],

Search Method	Top-1 Acc (Val)	Top-1 Acc (Train)	Pixel 6 EdgeTPU (ms)
One-stage	81.26	74.64	3.85
Two-stage	81.48 (+ <b>0.22</b> )	78.24 (+ <b>3.60</b> )	3.67 ( <b>-4.68%</b> )

**Table 3:** Comparison between one-stage and two-stage searches, highlighting accuracy improvements and latency reduction on Pixel 6 EdgeTPU.

GELU [16], LayerNorm [1] are not well supported on DSPs, with LayerNorm also lagging behind BatchNorm [23], and SE slow on accelerators.

*The Power of Simplicity:* Conventional components – depthwise and pointwise convolutions, ReLU [35], BatchNorm, and simple attention (e.g., MHSA) – demonstrate superior efficiency and hardware compatibility.

Based on these findings, we established a set of design principles:

- **Standard Components:** We prioritize widely supported elements for seamless deployment and hardware efficiency.
- **Flexible UIB Blocks:** Our novel searchable UIB building block allows for adaptable spatial and channel mixing, receptive field adjustments, and maximized computational utilization, facilitating a balanced compromise between efficiency and accuracy through Network Architecture Search (NAS).
- **Employ Straightforward Attention:** Our Mobile MQA mechanism prioritizes simplicity for optimal performance.

These principles allow MobileNetV4 to be mostly Pareto-optimal on all hardware evaluated. In the following, we detail our refined NAS recipe for UIB model search, outline specific search configurations for various MNv4-Conv model sizes, and explain the construction of hybrid models.

## 6.1 Refining NAS for Enhanced Architectures

To effectively instantiate the UIB blocks, we adopt TuNAS [3] with tailored enhancements for improved performance.

**Enhanced Search Strategy:** Our approach mitigates TuNAS’s bias towards smaller filters and expansion factors, attributed to parameter sharing, by implementing a two-stage search. This strategy addresses the variance in parameter counts between UIB’s depthwise layers and other search options.

*Coarse-Grained Search:* Initially, we focus on determining optimal filter sizes while maintaining fixed parameters: an inverted bottleneck block with a default expansion factor of 4 and a 3x3 depthwise kernel.

*Fine-Grained Search:* Building on the initial search’s outcomes, we search the configuration of UIB’s two depthwise layers (including their presence and kernel size of either 3x3 or 5x5), keeping the expansion factor constant at 4.

Table 3 demonstrates the enhanced efficiency and model quality achieved through our two-stage search compared to a conventional one-stage search, where a unified search space was explored in a single TuNAS pass.

**Enhancing TuNAS with Robust Training** The success of TuNAS hinges on accurately evaluating architecture quality, crucial for reward calculation and policy learning. Originally, TuNAS leverages ImageNet-1k for training the Super-

NAS Dataset	Top-1 Acc (Val/Train)	MACs	Params	Pixel 4 GPU	Pixel 6 CPU
ImageNet	82.4 / 72.9	7.2G	43.5M	59.2ms	70.4ms
JFT distill	82.3 / 74.0	6.2G	34.4M	51.0ms	67.3ms
Gain	-0.1 / +1.1	+13.9%	+20.9%	+13.9%	+4.4%

**Table 4:** Performance Boost from JFT Distillation: NAS Training on ImageNet-1k vs. JFT Data. Highlights efficiency improvements and slight accuracy differences.

Net, yet model performance on ImageNet is notably affected by data augmentation, regularization, and hyper-parameter choices. Given TuNAS’s evolving architecture samples, finding a stable set of hyper-parameters is challenging.

We address this with an offline distillation dataset, eliminating the need for extra augmentations and reducing sensitivity to regularization and optimization settings. The JFT distillation dataset, as detailed in Section 8, serves as our training set for TuNAS, showcasing notable improvements in Table 4. Acknowledging that depth-scaled models surpass width-scaled counterparts in extended training sessions [2], we extend TuNAS training to 750 epochs, yielding deeper, higher-quality models.

## 6.2 Optimization of MNv4 Models

We constructed MNv4-Conv models from NAS-optimized UIB blocks, tailoring them for specific resource constraints. More details are given in Appendix A. In line with other hybrid models, we found that adding attention to the last stages of convolution models is most effective. In MNv4-Hybrid models, we interlace Mobile MQA blocks with UIB blocks for enhanced performance. For comprehensive model specifications, refer to Appendix D.

## 7 Results

In this section, we demonstrate the mostly Pareto-optimal performance of MobileNet V4 (MNv4) models on both ImageNet-1K classification and COCO object detection.

### 7.1 ImageNet classification

**Experimental Setup:** To assess model architecture performance, we follow the standard protocol of training exclusively with the ImageNet-1k [11] training split and measuring Top-1 accuracy on its validation split. Our latency analysis spans a diverse and representative selection of mobile hardware, including ARM Cortex CPUs (Pixel 6, Samsung S23), Qualcomm Hexagon DSP (Pixel 4), ARM Mali GPU (Pixel 7), Qualcomm Snapdragon (S23 GPU), Apple Neural Engine, and Google EdgeTPU. Our complete training setting is detailed in the Appendix C.

In benchmarking, we compare our models against the leading efficient models, including both hybrid (MiT-EfficientViT [13], FastViT [42], NextViT [26]) and convolutional ones (MobileOne [43], ConvNext [32], and previous MobileNet

Model	Top-1	Latency (ms)								
		Params (M)	MACs (G)	Pixel 6 CPU	Pixel 8 EdgeTPU	iPhone 13 CoreML	Pixel 4 Hexagon	Pixel 7 GPU	Samsung S23 CPU	S23 GPU
MobileNet-V2-0.5x [36]	66	2.0	0.1	2.4	0.7	0.5	2.9	8.3	1.8	1.9
MobileNet-V3L-0.5x [18]	69.2	2.7	0.1	2.4	0.8	0.45	3.5	9.9	2.0	2.1
MobileOne-S0 [43]	71.4	2.1	0.3	4.2	0.7	0.5	2.9	10.7	3.0	1.7
MobileNet-V2 [36]	73.4	3.5	0.3	5.0	0.7	0.7	3.9	13.6	4.1	2.5
<b>MNv4-Conv-S</b>	<b>73.8</b>	<b>3.8</b>	<b>0.2</b>	<b>2.4</b>	<b>0.7</b>	<b>0.6</b>	<b>2.4</b>	<b>8.4</b>	<b>1.8</b>	<b>2.0</b>
MobileNet-V1 [20]	74.0	4.2	0.6	6.1	0.8	0.7	3.2	13.0	4.6	2.1
FastViT-T8 <sup>†</sup> [42]	75.6	3.6	0.7	49.3	1.3	0.7	<i>Failed</i>	40.7	43.6	24.7
MobileNet-V2-1.5x [36]	76.8	6.8	0.7	9.3	0.9	1.0	5.6	16.4	7.3	3.3
MultiHardware-MAX-1.5x [8]	77.9	8.9	0.8	9.8	1.0	-	5.7	23.2	-	4.1
MultiHardware-AVG-1.5x [8]	78.2	10.0	1.0	12.0	1.1	-	6.1	20.3	-	4.5
MobileNet-V2-2.0x [36]	78.4	11.2	1.1	13.9	1.1	1.5	6.9	19.1	10.6	4.2
MobileOne-S4 [43]	79.4	14.8	1.5	26.7	1.7	1.5	9.0	28.6	19.4	5.9
FastViT-S12 <sup>†</sup> [42]	79.8	8.8	1.8	83.0	1.8	1.6	<i>Failed</i>	75.0	69.2	47.0
MIT-EfficientViT-B1-r224 [13]	79.4	9.1	0.5	-	-	2.4	-	-	18.1	5.0
<b>MNv4-Conv-M</b>	<b>79.9</b>	<b>9.2</b>	<b>1.0</b>	<b>11.4</b>	<b>1.1</b>	<b>1.1</b>	<b>7.3</b>	<b>18.1</b>	<b>8.6</b>	<b>4.1</b>
FastViT-SA12 [42]	80.6	10.9	1.9	86.5	2.0	1.6	<i>Failed</i>	79.6	69.5	52.1
<b>MNv4-Hybrid-M</b>	<b>80.7</b>	<b>10.5</b>	<b>1.2</b>	<b>14.3</b>	<b>1.5</b>	-	<i>Failed</i>	<b>17.9</b>	<b>10.8</b>	<b>5.9</b>
FastViT-SA24 [42]	82.6	20.6	3.8	171.6	3.2	2.4	<i>Failed</i>	131.9	136.3	107.5
MIT-EfficientViT-B2-r256 [13]	82.7	24.0	2.1	-	-	5.4	-	-	64.9	9.5
<b>MNv4-Conv-L</b>	<b>82.9</b>	<b>31</b>	<b>5.9</b>	<b>59.9</b>	<b>2.4</b>	<b>3.0</b>	<b>20.8</b>	<b>37.6</b>	<b>43.0</b>	<b>13.2</b>
ConvNext-S [32]	83.1	50	8.7	314.9	3.7	-	<i>Failed</i>	45.2	243.9	18.5
NextViT-B [26]	83.2	44.8	8.3	-	-	-	-	-	-	-
MIT-EfficientViT-B3-r224 [13]	83.5	49.0	4.0	-	-	12.2	-	-	125.9	18.4
<b>MNv4-Hybrid-L</b>	<b>83.4</b>	<b>35.9</b>	<b>7.2</b>	<b>87.6</b>	<b>3.8</b>	-	<i>Failed</i>	<b>61.3</b>	<b>61.8</b>	<b>18.1</b>
FastViT-SA36 [42]	83.6	30.4	5.6	241.6	4.3	-	<i>Failed</i>	186.5	206.3	138.1

**Table 5: Classification results on ImageNet-1K [11], along with on-device benchmarks.** Median latency is reported. – indicates that we did not benchmark a model due to missing corresponding model file for a platform. *Failed* indicates that the model is not supported by the platform.

versions [19] [36] [18]), based on their reported Top-1 Accuracies and our latency evaluations. Notably, we’ve enhanced the MobileNet series (V1, V2, V3) with a modern training recipe, resulting in substantial accuracy improvements: a 3.4% increase to 74.0% for MobileNet V1, 1.4% to 73.4% for V2, and 0.3% to 75.5% for V3. These enhanced MobileNets baselines are used throughout the paper to isolate architectural advancements.

## Results:

Our results, illustrated in Figure 1 and detailed in Table 5, demonstrate that MNv4 models are mostly Pareto-optimal across a range of accuracy targets and mobile hardware, including CPUs, DSPs, GPUs, and specialized accelerators like the Apple Neural Engine and Google EdgeTPU.

On CPUs, MNv4 models notably outperform others, being approximately twice as fast as MobileNetV3 and several times faster compared to other models for equivalent accuracy targets. On EdgeTPUs, MNv4 models double the speed of MobileNet V3 at the same accuracy level. Specifically, the MNv4-Conv-M model is over 50% faster than both MobileOne-S4 and FastViT-S12, while also improving Top-1 accuracy by 1.5% over MobileNet V2 at comparable latencies. On S23 GPU and iPhone 13 CoreML (ANE), MNv4 models are mostly at the Pareto front. MIT-EfficientViT, the closest competitor on S23 GPU, has over

twice the latency as MNv4 on CoreML for the same accuracy. FastViT, optimized for the Apple Neural Engine, ranks second on CoreML but has more than 5 times the latency of MNv4 on S23 GPU. Like many hybrid models, MNv4-hybrid models are not compatible with DSPs. Nevertheless, MNv4-Conv models remain the top performers on DSP, emphasizing their leading compatibility and efficiency across diverse hardware platforms. MNv4-Conv models offer exceptional hardware compatibility and efficiency. This success highlights the strength of our UIB block, enhanced NAS recipe, and carefully designed search space. MNv4-Hybrid achieves excellent performance on CPUs and accelerators, demonstrating the cross-platform efficiency of our Mobile MQA design.

Universality is crucial for mobile models, requiring them to perform optimally across diverse hardware platforms. Our evaluation highlights the challenge existing models face in achieving this goal. MobileNet V3 shows decent performance on CPUs but falls short on EdgeTPUs, DSPs, and GPUs. FastViT performs well on the Apple Neural Engine but struggles on CPUs and GPUs. EfficientViT has good performance on GPUs but does not do as well on the Apple Neural Engine. In contrast, MNv4-Conv models exhibit exceptional compatibility and achieve universal mostly Pareto-optimal performance across a wide range of hardware, including CPUs, GPUs, the Apple Neural Engine, and Google EdgeTPUs. This versatility ensures MNv4-Conv models can be deployed seamlessly across the Mobile Ecosystems without any platform-specific adjustments, setting a new benchmark for mobile model universality.

## 7.2 COCO Object Detection

**Experimental Setup:** We evaluate the effectiveness of MNv4 backbones for object detection tasks, on the COCO 17 [31] dataset. We compare M-sized MNv4 backbones against SOTA efficient backbones with a similar number of MACs. For each backbone, we build an object detector using the RetinaNet [30] framework. We attach a 256-d FPN [29] decoder to the P3 - P7 endpoints, and a 256-d prediction head, with 4 convolutional layers. As usual for mobile detectors, we employ depth-separable convolutions to reduce the computational complexity of both the FPN decoder and the box prediction head. We train all models on the COCO 17 [31] training set for 600-epochs. All images are resized to  $384px$  and augmented using random horizontal flip, random scale, as well as Randaug [9]. We exclude Shear and Rotate augmentations from Randaug, as those deformations deteriorate small-objects detection AP. Training is performed using a 2048 batch size, Adam [24], and a L2 weight decay of 0.00003. We use a cosine learning rate schedule with 24 epochs warm-up, and separately tune the learning rate for each model. For all baselines, we set the filter multiplier so that MACs are roughly comparable. Following classification experiments, MobileNet V4 backbones are trained using a stochastic drop [22] rate of 0.2. All MobileNet baselines were trained using the official Tensorflow Model Garden [17] implementation. We re-implemented EfficientFormer in Tensorflow.

**Results:** Experimental results are reported in Table 6. Parameters, MACs and benchmarks are computed using the entire detector at the  $384px$  input

Backbone	COCO		MACs	Params	Pixel 6 CPU
	Val AP	(G)	(M)	latency (ms)	
EfficientFormer L1 [28]	29.5	6.54	12.77	84.3	
MobileNet v1 @ 1.5 [19]	31.0	6.68	9.05	66.4	
<b>MNv4-Conv-M</b>	<b>32.6</b>	<b>5.06</b>	<b>9.79</b>	<b>51.3</b>	
MobileNet Multi-AVG @ 1.5 [8]	32.7	5.42	9.51	58.1	
MobileNet v2 @ 2.0 [36]	32.9	5.81	10.15	66.4	
MobileNet v3 Large [18] @ 2.0	33.2	4.99	17.92	59.9	
<b>MNv4-Hybrid-M</b>	<b>34.0</b>	<b>5.62</b>	<b>11.15</b>	<b>60.5</b>	

**Table 6:** Object detection results on the COCO-17 [31] Val. set. The width-multiplier is reported next to the MobileNet backbones that were scaled-up.

resolution. The medium-size convolutional-only MNv4-Conv-M detector achieves 32.6% AP, similar to MobileNet Multi-AVG and MobileNet v2. However, the Pixel 6 CPU latency for this model is 12% lower than MobileNet Multi-AVG, and 23% lower than MobileNet v2. With an 18% increase in Pixel 6 CPU latency, adding Mobile MQA blocks increases the MNv4-Hybrid-M detector’s AP by +1.6% over MNv4-Conv-M, demonstrating MNv4’s effectiveness and efficiency in its Hybrid form for tasks like object detection.

## 8 Enhanced distillation recipe

Complementing architectural innovation, distillation is a powerful tool for enhancing machine learning efficiency. Its benefits are especially pronounced for mobile models, potentially offering several-fold efficiency gains within tight deployment constraints. Building upon the strong Patient Teacher distillation baseline [4], we introduce two novel techniques to further boost performance.

**Dynamic Dataset Mixing:** Data augmentation is crucial for distillation performance. While prior methods rely on a fixed augmentation sequence, we find that dynamically mixing multiple datasets with diverse augmentation strategies leads to superior distillation outcomes. We experimented with three key distillation datasets:

- $\mathcal{D}_1$  : Inception Crop [39] followed by RandAugment [10] l2m9 applied to 500 ImageNet-1k replicas.
- $\mathcal{D}_2$  : Inception Crop followed by extreme Mixup [51] applied to 1000 ImageNet-1k replicas (mirroring the Patient Teacher approach).
- $\mathcal{D}_1 + \mathcal{D}_2$  : A dynamic mixture of  $\mathcal{D}_1$  and  $\mathcal{D}_2$  during training.

Our results in table 7 show that  $\mathcal{D}_2$  outperforms  $\mathcal{D}_1$  in student accuracy (84.1% vs. 83.8%). However, dynamically mixing datasets ( $\mathcal{D}_1 + \mathcal{D}_2$ ) elevates accuracy to 84.4% (+0.3%). This finding suggests that dataset mixing expands the augmented image space, increasing difficulty and diversity, which ultimately leads to improved student performance.

**JFT Data Augmentation:** To increase training data volume, we add in-domain, class-balanced data by resampling the JFT-300M [38] dataset to 130K images per class (130M total). Following the Noisy Student [48] protocol and using EfficientNet-B0 trained on ImageNet-1K, we select images with a relevance

Dataset	Data source	Augmentations	Mixing Ratio	Top-1 Acc (Val/Train)	
				400 epochs	2000 epochs
$\mathcal{D}_1$	1000× ImageNet-1k	Inception Crop & RandAug l2m9	-	83.8/86.6	-
$\mathcal{D}_2$ (SOTA [4])	1000× ImageNet-1k	Inception Crop & Extreme Mixup	-	84.1/85.6	-
$\mathcal{D}_3$	10× JFT subset	Inception Crop & RandAug l2m5	-	81.8/84.1	-
<b>Ours: <math>\mathcal{D}_1 + \mathcal{D}_2</math></b>			1:1	<b>84.4/85.0 (+0.3)</b>	-
<b>Ours: <math>\mathcal{D}_2 + \mathcal{D}_3</math></b>			1:1	<b>84.7/82.7 (+0.6)</b>	-
<b>Ours: <math>\mathcal{D}_1 + \mathcal{D}_2 + \mathcal{D}_3</math></b>			1:1:2	<b>84.9/82.6 (+0.8)</b>	85.9/85.5 (+1.8)

**Table 7:** Distillation results using MNv4-Conv-L as student, highlighting gains over SOTA and marking our contributions explicitly.

Model	IN-1k Only	SOTA Distill [4]	<b>Our Distill</b>	<b>Our Gain Over</b> IN-1k / SOTA
MNv4-Conv-S	73.8	-	<b>75.5</b>	+1.7 / -
MNv4-Conv-M	79.9	81.5	<b>82.7</b>	+2.8 / +1.2
MNv4-Hybrid-M	80.7	82.7	<b>83.7</b>	+3.0 / +1.0
MNv4-Conv-L	82.9	84.4	<b>85.9</b>	+3.0 / +1.5
MNv4-Hybrid-L	83.4	85.7	<b>86.6</b>	+3.2 / +0.9

**Table 8: Top-1 Accuracy Comparison Across Training Approaches:** This table contrasts baseline ImageNet-1k training, State-of-the-Art (SOTA) distillation, and our distillation method.

threshold above 0.3. For classes with abundant data, we choose the top 130K images; for rare classes, we replicate images for balance. This dataset is replicated 10x. Due to JFT’s complexity, we apply weaker augmentations (Inception Crop + RandAugment l2m5). This forms distillation dataset  $\mathcal{D}_3$ . Table 7 show that using JFT alone ( $\mathcal{D}_3$ ) yields a 2% accuracy drop. However, combining JFT with ImageNet data results in a 0.6% improvement, demonstrating the value of additional data for generalization.

**Our distillation recipe:** Our combined distillation recipe dynamically mixes datasets  $\mathcal{D}_1$ ,  $\mathcal{D}_2$ , and  $\mathcal{D}_3$  for diverse augmentations and leverages class-balanced JFT data. As shown in Table 7 and 8, our method achieves consistent improvements of over 0.8% top-1 accuracy compared to the previous SOTA [4]. Training an MNv4-Conv-L student model for 2000 epochs yields 85.9% top-1 accuracy. This demonstrates the effectiveness of our approach: the student is 15x smaller in parameters and 48x smaller in MACs than its teacher EfficientNet-L2, yet suffers only a 1.6% accuracy drop. When combined distillation with pre-training on JFT, MNv4-Conv-Hybrid reaches 87.0% top-1 accuracy.

## 9 Conclusion

In this paper, we presented MobileNetV4, a series of universal, highly efficient models tuned to run efficiently across the mobile ecosystem. We leverage multiple advances to make MobileNetV4 mostly-Pareto-optimal on all mobile CPUs, GPUs, DSPs and specialized accelerators, a characteristic not found in any other

models tested. We introduced the new Universal Inverted Bottleneck and Mobile MQA layers and combined them with improved NAS recipes. Combining these with a novel, state of the art distillation approach, we achieve 87% ImageNet-1K accuracy at 3.8ms latency on Pixel 8 EdgeTPU advancing the state of the art of mobile computer vision. Additionally, we introduced a theoretical framework and analysis to understand what makes models universal on heterogeneous devices pointing the way to future designs. We hope that the novel contributions and analysis framework further spur advances in mobile computer vision.

## 10 Acknowledgements

We would like to thank Tammo Spalink, Yeqing Li, Bob Muniz, David Wood, and Lynn Nguyen for their support while developing this work.

## References

1. Jimmy Lei Ba, Jamie Ryan Kiros, and Geoffrey E Hinton. Layer normalization. *arXiv preprint arXiv:1607.06450*, 2016.
2. Irwan Bello, William Fedus, Xianzhi Du, Ekin Dogus Cubuk, Aravind Srinivas, Tsung-Yi Lin, Jonathon Shlens, and Barret Zoph. Revisiting resnets: Improved training and scaling strategies. *Advances in Neural Information Processing Systems*, 34:22614–22627, 2021.
3. Gabriel Bender, Hanxiao Liu, Bo Chen, Grace Chu, Shuyang Cheng, Pieter-Jan Kindermans, and Quoc V. Le. Can weight sharing outperform random architecture search? an investigation with tunas. In *The IEEE/CVF Conference on Computer Vision and Pattern Recognition (CVPR)*, June 2020.
4. Lucas Beyer, Xiaohua Zhai, Amélie Royer, Larisa Markeeva, Rohan Anil, and Alexander Kolesnikov. Knowledge distillation: A good teacher is patient and consistent. In *Proceedings of the IEEE/CVF conference on computer vision and pattern recognition*, pages 10925–10934, 2022.
5. Han Cai, Chuang Gan, Tianzhe Wang, Zhekai Zhang, and Song Han. Once-for-all: Train one network and specialize it for efficient deployment. *arXiv preprint arXiv:1908.09791*, 2019.
6. Yinpeng Chen, Xiyang Dai, Dongdong Chen, Mengchen Liu, Xiaoyi Dong, Lu Yuan, and Zicheng Liu. Mobile-former: Bridging mobilenet and transformer. In *Proceedings of the IEEE/CVF Conference on Computer Vision and Pattern Recognition*, pages 5270–5279, 2022.
7. Aakanksha Chowdhery, Sharan Narang, Jacob Devlin, Maarten Bosma, Gaurav Mishra, Adam Roberts, Paul Barham, Hyung Won Chung, Charles Sutton, Sebastian Gehrmann, et al. Palm: Scaling language modeling with pathways. *arXiv preprint arXiv:2204.02311*, 2022.
8. Grace Chu, Okan Arikan, Gabriel Bender, Weijun Wang, Achille Brighton, Pieter-Jan Kindermans, Hanxiao Liu, Berkin Akin, Suyog Gupta, and Andrew Howard. Discovering multi-hardware mobile models via architecture search. In *IEEE Conference on Computer Vision and Pattern Recognition Workshops, CVPR Workshops 2021, virtual, June 19-25, 2021*, pages 3022–3031. Computer Vision Foundation / IEEE, 2021.

9. Ekin Dogus Cubuk, Barret Zoph, Jonathon Shlens, and Quoc Le. Randaugment: Practical automated data augmentation with a reduced search space. In Hugo Larochelle, Marc’Aurelio Ranzato, Raia Hadsell, Maria-Florina Balcan, and Hsuan-Tien Lin, editors, *Advances in Neural Information Processing Systems 33: Annual Conference on Neural Information Processing Systems 2020, NeurIPS 2020, December 6-12, 2020, virtual*, 2020.
10. Ekin D Cubuk, Barret Zoph, Jonathon Shlens, and Quoc V Le. Randaugment: Practical automated data augmentation with a reduced search space. In *Proceedings of the IEEE/CVF conference on computer vision and pattern recognition workshops*, pages 702–703, 2020.
11. J. Deng, W. Dong, R. Socher, L. Li, Kai Li, and Li Fei-Fei. Imagenet: A large-scale hierarchical image database. In *2009 IEEE Conference on Computer Vision and Pattern Recognition*, pages 248–255, June 2009.
12. Alexey Dosovitskiy, Lucas Beyer, Alexander Kolesnikov, Dirk Weissenborn, Xiuhua Zhai, Thomas Unterthiner, Mostafa Dehghani, Matthias Minderer, Georg Heigold, Sylvain Gelly, et al. An image is worth 16x16 words: Transformers for image recognition at scale. *arXiv preprint arXiv:2010.11929*, 2020.
13. Han Cai et al. Efficientvit: Lightweight multi-scale attention for high-resolution dense prediction. In *ICCV*, 2023.
14. Xinyu Liu et al. Efficientvit: Memory efficient vision transformer with cascaded group attention. In *CVPR*, 2023.
15. Jianyuan Guo, Kai Han, Han Wu, Yehui Tang, Xinghao Chen, Yunhe Wang, and Chang Xu. Cmt: Convolutional neural networks meet vision transformers. In *Proceedings of the IEEE/CVF Conference on Computer Vision and Pattern Recognition*, pages 12175–12185, 2022.
16. Dan Hendrycks and Kevin Gimpel. Gaussian error linear units (gelus). *arXiv preprint arXiv:1606.08415*, 2016.
17. Xianzhi Du Yeqing Li Abdullah Rashwan Le Hou Pengchong Jin Fan Yang Frederick Liu Jaeyoun Kim Hongkun Yu, Chen Chen and Jing Li. TensorFlow Model Garden. <https://github.com/tensorflow/models>, 2020.
18. Andrew Howard, Mark Sandler, Grace Chu, Liang-Chieh Chen, Bo Chen, Mingxing Tan, Weijun Wang, Yukun Zhu, Ruoming Pang, Vijay Vasudevan, Quoc V. Le, and Hartwig Adam. Searching for mobilenetv3. *CoRR*, abs/1905.02244, 2019.
19. Andrew G. Howard, Menglong Zhu, Bo Chen, Dmitry Kalenichenko, Weijun Wang, Tobias Weyand, Marco Andreetto, and Hartwig Adam. Mobilenets: Efficient convolutional neural networks for mobile vision applications. *CoRR*, abs/1704.04861, 2017.
20. Andrew G Howard, Menglong Zhu, Bo Chen, Dmitry Kalenichenko, Weijun Wang, Tobias Weyand, Marco Andreetto, and Hartwig Adam. Mobilenets: Efficient convolutional neural networks for mobile vision applications. *arXiv preprint arXiv:1704.04861*, 2017.
21. Jie Hu, Li Shen, and Gang Sun. Squeeze-and-excitation networks. In *Proceedings of the IEEE conference on computer vision and pattern recognition*, pages 7132–7141, 2018.
22. Gao Huang, Yu Sun, Zhuang Liu, Daniel Sedra, and Kilian Q Weinberger. Deep networks with stochastic depth. In *Computer Vision—ECCV 2016: 14th European Conference, Amsterdam, The Netherlands, October 11–14, 2016, Proceedings, Part IV 14*, pages 646–661. Springer, 2016.
23. Sergey Ioffe and Christian Szegedy. Batch normalization: Accelerating deep network training by reducing internal covariate shift. In *International conference on machine learning*, pages 448–456. pmlr, 2015.

24. Diederik Kingma and Jimmy Ba. Adam: A method for stochastic optimization. In *International Conference on Learning Representations (ICLR)*, San Diego, CA, USA, 2015.
25. Ariel N Lee, Cole J Hunter, and Nataniel Ruiz. Platypus: Quick, cheap, and powerful refinement of llms. *arXiv preprint arXiv:2308.07317*, 2023.
26. Jiashi Li, Xin Xia, Wei Li, Huixia Li, Xing Wang, Xuefeng Xiao, Rui Wang, Min Zheng, and Xin Pan. Next-vit: Next generation vision transformer for efficient deployment in realistic industrial scenarios. *arXiv preprint arXiv:2207.05501*, 2022.
27. Yanyu Li, Ju Hu, Yang Wen, Georgios Evangelidis, Kamyar Salahi, Yanzhi Wang, Sergey Tulyakov, and Jian Ren. Rethinking vision transformers for mobilenet size and speed. In *Proceedings of the IEEE/CVF International Conference on Computer Vision*, pages 16889–16900, 2023.
28. Yanyu Li, Geng Yuan, Yang Wen, Ju Hu, Georgios Evangelidis, Sergey Tulyakov, Yanzhi Wang, and Jian Ren. Efficientformer: Vision transformers at mobilenet speed. In *NeurIPS*, 2022.
29. Tsung-Yi Lin, Piotr Dollár, Ross B. Girshick, Kaiming He, Bharath Hariharan, and Serge J. Belongie. Feature pyramid networks for object detection. In *2017 IEEE Conference on Computer Vision and Pattern Recognition, CVPR 2017, Honolulu, HI, USA, July 21-26, 2017*, pages 936–944. IEEE Computer Society, 2017.
30. Tsung-Yi Lin, Priya Goyal, Ross B. Girshick, Kaiming He, and Piotr Dollár. Focal loss for dense object detection. In *IEEE International Conference on Computer Vision, ICCV 2017, Venice, Italy, October 22-29, 2017*, pages 2999–3007. IEEE Computer Society, 2017.
31. Tsung-Yi Lin, Michael Maire, Serge J. Belongie, James Hays, Pietro Perona, Deva Ramanan, Piotr Dollár, and C. Lawrence Zitnick. Microsoft COCO: common objects in context. In David J. Fleet, Tomás Pajdla, Bernt Schiele, and Tinne Tuytelaars, editors, *Computer Vision - ECCV 2014 - 13th European Conference, Zurich, Switzerland, September 6-12, 2014, Proceedings, Part V*, volume 8693 of *Lecture Notes in Computer Science*, pages 740–755. Springer, 2014.
32. Zhuang Liu, Hanzi Mao, Chao-Yuan Wu, Christoph Feichtenhofer, Trevor Darrell, and Saining Xie. A convnet for the 2020s. In *IEEE/CVF Conference on Computer Vision and Pattern Recognition, CVPR 2022, New Orleans, LA, USA, June 18-24, 2022*, pages 11966–11976. IEEE, 2022.
33. Sachin Mehta and Mohammad Rastegari. Mobilevit: light-weight, general-purpose, and mobile-friendly vision transformer. *arXiv preprint arXiv:2110.02178*, 2021.
34. Sachin Mehta and Mohammad Rastegari. Separable self-attention for mobile vision transformers. *arXiv preprint arXiv:2206.02680*, 2022.
35. Vinod Nair and Geoffrey E Hinton. Rectified linear units improve restricted boltzmann machines. In *Proceedings of the 27th international conference on machine learning (ICML-10)*, pages 807–814, 2010.
36. Mark Sandler, Andrew G. Howard, Menglong Zhu, Andrey Zhmoginov, and Liang-Chieh Chen. Mobilenetv2: Inverted residuals and linear bottlenecks. *CoRR*, abs/1801.04381, 2018.
37. Noam Shazeer. Fast transformer decoding: One write-head is all you need. *arXiv preprint arXiv:1911.02150*, 2019.
38. Chen Sun, Abhinav Shrivastava, Saurabh Singh, and Abhinav Gupta. Revisiting unreasonable effectiveness of data in deep learning era. In *Proceedings of the IEEE international conference on computer vision*, pages 843–852, 2017.
39. Christian Szegedy, Vincent Vanhoucke, Sergey Ioffe, Jon Shlens, and Zbigniew Wojna. Rethinking the inception architecture for computer vision. In *Proceedings of the IEEE conference on computer vision and pattern recognition*, pages 2818–2826, 2016.

40. Mingxing Tan, Bo Chen, Ruoming Pang, Vijay Vasudevan, and Quoc V. Le. Mnasnet: Platform-aware neural architecture search for mobile. *CoRR*, abs/1807.11626, 2018.
41. Mingxing Tan and Quoc Le. Efficientnet: Rethinking model scaling for convolutional neural networks. In *International conference on machine learning*, pages 6105–6114. PMLR, 2019.
42. Pavan Kumar Anasosalu Vasu, James Gabriel, Jeff Zhu, Oncel Tuzel, and Anurag Ranjan. Fastvit: A fast hybrid vision transformer using structural reparameterization. *arXiv preprint arXiv:2303.14189*, 2023.
43. Pavan Kumar Anasosalu Vasu, James Gabriel, Jeff Zhu, Oncel Tuzel, and Anurag Ranjan. Mobileone: An improved one millisecond mobile backbone. In *Proceedings of the IEEE/CVF Conference on Computer Vision and Pattern Recognition*, pages 7907–7917, 2023.
44. Ashish Vaswani, Noam Shazeer, Niki Parmar, Jakob Uszkoreit, Llion Jones, Aidan N Gomez, Łukasz Kaiser, and Illia Polosukhin. Attention is all you need. *Advances in neural information processing systems*, 30, 2017.
45. Wenhai Wang, Enze Xie, Xiang Li, Deng-Ping Fan, Kaitao Song, Ding Liang, Tong Lu, Ping Luo, and Ling Shao. Pyramid vision transformer: A versatile backbone for dense prediction without convolutions. In *Proceedings of the IEEE/CVF international conference on computer vision*, pages 568–578, 2021.
46. Samuel Williams, Andrew Waterman, and David Patterson. Roofline: an insightful visual performance model for multicore architectures. *Communications of the ACM*, 52(4):65–76, 2009.
47. Bichen Wu, Xiaoliang Dai, Peizhao Zhang, Yanghan Wang, Fei Sun, Yiming Wu, Yuandong Tian, Peter Vajda, Yangqing Jia, and Kurt Keutzer. Fbnet: Hardware-aware efficient convnet design via differentiable neural architecture search. *CoRR*, abs/1812.03443, 2018.
48. Qizhe Xie, Minh-Thang Luong, Eduard Hovy, and Quoc V Le. Self-training with noisy student improves imagenet classification. In *Proceedings of the IEEE/CVF conference on computer vision and pattern recognition*, pages 10687–10698, 2020.
49. Tien-Ju Yang, Andrew G. Howard, Bo Chen, Xiao Zhang, Alec Go, Vivienne Sze, and Hartwig Adam. Netadapt: Platform-aware neural network adaptation for mobile applications. *CoRR*, abs/1804.03230, 2018.
50. Sangdoon Yun, Dongyoon Han, Seong Joon Oh, Sanghyuk Chun, Junsuk Choe, and Youngjoon Yoo. Cutmix: Regularization strategy to train strong classifiers with localizable features. In *Proceedings of the IEEE/CVF international conference on computer vision*, pages 6023–6032, 2019.
51. Hongyi Zhang, Moustapha Cisse, Yann N Dauphin, and David Lopez-Paz. mixup: Beyond empirical risk minimization. *arXiv preprint arXiv:1710.09412*, 2017.
52. Xiangyu Zhang, Xinyu Zhou, Mengxiao Lin, and Jian Sun. Shufflenet: An extremely efficient convolutional neural network for mobile devices. *CoRR*, abs/1707.01083, 2017.

## A Search space details

The following is how we construct the search space for NAS.

### Search Space Construction:

- *Fixed Initial Layers:* We started with a Conv2D layer (3x3 kernel, stride 2) in the first stage for quick resolution reduction, followed by NAS-optimized FusedIB blocks (stride 2) in the second stage to balance between efficiency and accuracy.
- *NAS-Driven Optimization:* The NAS process precisely determined the ideal number of UIB blocks and parameter instantiations across the remaining four stages, ensuring an optimal structure for performance.
- *Fixed Head Layers:* We use same head layers configuration as MobileNet V3.

Observing that pointwise convolutions within UIB blocks tend to exhibit low operational intensity at higher resolutions, we prioritized operations with higher computational density in the initial layers to balance efficiency and accuracy.

### Our optimization targets:

- MNv4-Conv-S: Dual goals—285M MACs and 0.2ms latency (Pixel 6 EdgeTPU, 224px inputs).
- MNv4-Conv-M: 0.6ms latency (Pixel 6 EdgeTPU, 256px inputs).
- MNv4-Conv-L: Dual latency goals of 2.3ms (Pixel 6 EdgeTPU) and 2.0ms (Pixel 7 EdgeTPU) with 384px inputs.

To be noted, by restricting our search space to components with well-correlated cost models across devices, we found that EdgeTPU latency optimization directly yields universally efficient models, as demonstrated in later sections.

## B Benchmarking methodology

We applied a consistent benchmarking strategy across various mobile platforms, with an exception for the Apple Neural Engine. To enhance efficiency, models were converted to TensorFlow Lite format and quantized to INT8 for mobile CPUs, Hexagon, and EdgeTPUs, while FP16 was used for mobile GPUs. We run each model 1000 times and take the mean latency of those runs. We then repeat that process 5 times for each model and report the median of means. To optimize performance, we set the CPU affinity to the fastest core and use the XNNPACK backend for CPU evaluations. In contrast, for benchmarks on the Apple Neural Engine (conducted on an iPhone 13 with iOS 16.6.1, CoreMLTools 7.1, and Xcode 15.0.1 for profiling), PyTorch models were converted to CoreML’s MLProgram format in Float16 precision, with float16 MultiArray inputs to minimize input copying.

## C Training setup for ImageNet-1k classification

To enhance model performance, our training recipe incorporates widely adopted data augmentation techniques and regularization methods. For data augmenta-

	Conv-S	Conv-M	Hybrid-M	Conv-L	Hybrid-L
Batch size	4096	4096	16384	16384	16384
Peak learning rate	0.002	0.004	0.016	0.004	0.01
Warm-up epochs	5	5	20	20	20
Training epochs	9600	500	500	500	500
AdamW weight decay	0.01	0.1	0.1	0.2	0.2
AdamW $\beta_1$	0.6	0.9	0.9	0.9	0.9
AdamW $\beta_2$	0.999	0.999	0.999	0.999	0.999
AdamW $\epsilon$	$10^{-6}$	$10^{-7}$	$10^{-7}$	$10^{-7}$	$10^{-7}$
EMA decay	0.9999	-	-	-	-
L2-regularization	$10^{-5}$	-	-	-	-
Gradient clipping	-	-	-	-	-
Label smoothing	0.1	0.1	0.1	0.1	0.1
Dropout	0.3	0.2	0.2	0.2	0.2
Peak Stochastic Depth drop rate	0	0.075	0.075	0.35	0.35
RandAugment probability	0.5	0.7	0.7	1.0	1.0
RandAugment layers	2	2	2	2	2
RandAugment magnitude	9	15	15	15	15
RandAugment excluded ops	Cutout	Cutout	Cutout	Cutout	Cutout
Mixup/Cutmix probability	-	-	-	0.3	0.3
Mixup $\alpha$	-	-	-	0.8	0.8
Cutmix $\alpha$	-	-	-	1.0	1.0
Mixup/Cutmix switch probability	-	-	-	0.5	0.5

**Table 9:** Training hyper-parameters for ImageNet-1k classification.

tion, we use Inception Crop [39], horizontal flip, RandAugment [9], Mixup [51], and CutMix [50]. For regularization, we apply L2 normalization and stochastic depth drop [22]. The intensity of augmentation and regularization is adjusted according to model size, as detailed in Table 9.

## D Model details

The architecture details of our MNv4 models are described from Table 10 to Table 14.

Now, let’s examine the details of the TuNAS-optimized MNv4-Conv models. TuNAS optimized macro architecture strategically combines four UIB instantiations: Extra DW, ConvNext, IB, and FFN. This combination demonstrates the flexibility of UIB and the importance of using different instantiation blocks in different stages of the network. Specifically, at the start of each searchable stage, where the spatial resolution significantly drops, ExtraDW emerges as the preferred choice. The design of duo depthwise layers in ExtraDW helps to enlarge the receptive field, enhances spatial mixing, and effectively mitigates resolution loss. Similarly, ExtraDW is frequently selected in the early stages of MNv4-Conv models for similar reasons. For the final layers, where preceding layers have conducted substantial spatial mixing, FFN and ConvNext are chosen because channel mixing provides a larger incremental gain.

Input	Block	DW $K_1$	DW $K_2$	Expanded Dim	Output Dim	Stride
$224^2 \times 3$	Conv2D	-	$3 \times 3$	-	32	2
$112^2 \times 32$	FusedIB	-	$3 \times 3$	32	32	2
$56^2 \times 32$	FusedIB	-	$3 \times 3$	96	64	2
$28^2 \times 64$	ExtraDW	$5 \times 5$	$5 \times 5$	192	96	2
$14^2 \times 96$	IB	-	$3 \times 3$	192	96	1
$14^2 \times 96$	IB	-	$3 \times 3$	192	96	1
$14^2 \times 96$	IB	-	$3 \times 3$	192	96	1
$14^2 \times 96$	IB	-	$3 \times 3$	192	96	1
$14^2 \times 96$	ConvNext	$3 \times 3$	-	384	96	1
$14^2 \times 96$	ExtraDW	$3 \times 3$	$3 \times 3$	576	128	2
$7^2 \times 128$	ExtraDW	$5 \times 5$	$5 \times 5$	512	128	1
$7^2 \times 128$	IB	-	$5 \times 5$	512	128	1
$7^2 \times 128$	IB	-	$5 \times 5$	384	128	1
$7^2 \times 128$	IB	-	$3 \times 3$	512	128	1
$7^2 \times 128$	IB	-	$3 \times 3$	512	128	1
$7^2 \times 128$	Conv2D	-	$1 \times 1$	-	960	1
$7^2 \times 960$	AvgPool	-	$7 \times 7$	-	960	1
$1^2 \times 960$	Conv2D	-	$1 \times 1$	-	1280	1
$1^2 \times 1280$	Conv2D	-	$1 \times 1$	-	1000	1

Table 10: Architecture specification of MNv4-Conv-S.

Input	Block	DW $K_1$	DW $K_2$	Expanded Dim	Output Dim	Stride
$256^2 \times 3$	Conv2D	-	$3 \times 3$	-	32	2
$128^2 \times 32$	FusedIB	-	$3 \times 3$	128	48	2
$64^2 \times 48$	ExtraDW	$3 \times 3$	$5 \times 5$	192	80	2
$32^2 \times 80$	ExtraDW	$3 \times 3$	$3 \times 3$	160	80	1
$32^2 \times 80$	ExtraDW	$3 \times 3$	$5 \times 5$	480	160	2
$16^2 \times 160$	ExtraDW	$3 \times 3$	$3 \times 3$	640	160	1
$16^2 \times 160$	ExtraDW	$3 \times 3$	$3 \times 3$	640	160	1
$16^2 \times 160$	ExtraDW	$3 \times 3$	$5 \times 5$	640	160	1
$16^2 \times 160$	ExtraDW	$3 \times 3$	$3 \times 3$	640	160	1
$16^2 \times 160$	ConvNext	$3 \times 3$	-	640	160	1
$16^2 \times 160$	FFN	-	-	320	160	1
$16^2 \times 160$	ConvNext	$3 \times 3$	-	640	160	1
$16^2 \times 160$	ExtraDW	$5 \times 5$	$5 \times 5$	960	256	2
$8^2 \times 256$	ExtraDW	$5 \times 5$	$5 \times 5$	1024	256	1
$8^2 \times 256$	ExtraDW	$3 \times 3$	$5 \times 5$	1024	256	1
$8^2 \times 256$	ExtraDW	$3 \times 3$	$5 \times 5$	1024	256	1
$8^2 \times 256$	FFN	-	-	1024	256	1
$8^2 \times 256$	ConvNext	$3 \times 3$	-	1024	256	1
$8^2 \times 256$	ExtraDW	$3 \times 3$	$5 \times 5$	512	256	1
$8^2 \times 256$	ExtraDW	$5 \times 5$	$5 \times 5$	1024	256	1
$8^2 \times 256$	FFN	-	-	1024	256	1
$8^2 \times 256$	FFN	-	-	1024	256	1
$8^2 \times 256$	ConvNext	$5 \times 5$	-	512	256	1
$8^2 \times 256$	Conv2D	-	$1 \times 1$	-	960	1
$8^2 \times 960$	AvgPool	-	$8 \times 8$	-	960	1
$1^2 \times 960$	Conv2D	-	$1 \times 1$	-	1280	1
$1^2 \times 1280$	Conv2D	-	$1 \times 1$	-	1000	1

Table 11: Architecture specification of MNv4-Conv-M.

Input	Block	DW $K_1$	DW $K_2$	Expanded Dim	Output Dim	Stride
$256^2 \times 3$	Conv2D	-	$3 \times 3$	-	32	2
$128^2 \times 32$	FusedIB	-	$3 \times 3$	128	48	2
$64^2 \times 48$	ExtraDW	$3 \times 3$	$5 \times 5$	192	80	2
$32^2 \times 80$	ExtraDW	$3 \times 3$	$3 \times 3$	160	80	1
$32^2 \times 80$	ExtraDW	$3 \times 3$	$5 \times 5$	480	160	2
$16^2 \times 160$	ExtraDW	$3 \times 3$	$3 \times 3$	640	160	1
$16^2 \times 160$	ExtraDW	$3 \times 3$	$3 \times 3$	640	160	1
$16^2 \times 160$	ExtraDW	$3 \times 3$	$5 \times 5$	640	160	1
$16^2 \times 160$	Mobile-MQA	-	-	-	160	1
$16^2 \times 160$	ExtraDW	$3 \times 3$	$3 \times 3$	640	160	1
$16^2 \times 160$	Mobile-MQA	-	-	-	160	1
$16^2 \times 160$	ConvNext	$3 \times 3$	-	640	160	1
$16^2 \times 160$	Mobile-MQA	-	-	-	160	1
$16^2 \times 160$	FFN	-	-	640	160	1
$16^2 \times 160$	Mobile-MQA	-	-	-	160	1
$16^2 \times 160$	ConvNext	$3 \times 3$	-	640	160	1
$16^2 \times 160$	ExtraDW	$5 \times 5$	$5 \times 5$	960	256	2
$8^2 \times 256$	ExtraDW	$5 \times 5$	$5 \times 5$	1024	256	1
$8^2 \times 256$	ExtraDW	$3 \times 3$	$5 \times 5$	1024	256	1
$8^2 \times 256$	ExtraDW	$3 \times 3$	$5 \times 5$	1024	256	1
$8^2 \times 256$	FFN	-	-	1024	256	1
$8^2 \times 256$	ConvNext	$3 \times 3$	-	1024	256	1
$8^2 \times 256$	ExtraDW	$3 \times 3$	$5 \times 5$	512	256	1
$8^2 \times 256$	Mobile-MQA	-	-	-	256	1
$8^2 \times 256$	ExtraDW	$5 \times 5$	$5 \times 5$	1024	256	1
$8^2 \times 256$	Mobile-MQA	-	-	-	256	1
$8^2 \times 256$	FFN	-	-	1024	256	1
$8^2 \times 256$	Mobile-MQA	-	-	-	256	1
$8^2 \times 256$	FFN	-	-	1024	256	1
$8^2 \times 256$	Mobile-MQA	-	-	-	256	1
$8^2 \times 256$	ConvNext	$5 \times 5$	-	1024	256	1
$8^2 \times 256$	Conv2D	-	$1 \times 1$	-	960	1
$8^2 \times 960$	AvgPool	-	$8 \times 8$	-	960	1
$1^2 \times 960$	Conv2D	-	$1 \times 1$	-	1280	1
$1^2 \times 1280$	Conv2D	-	$1 \times 1$	-	1000	1

Table 12: Architecture specification of MNv4-Hybrid-M.

Input	Block	DW $K_1$	DW $K_2$	Expanded Dim	Output Dim	Stride
$384^2 \times 3$	Conv2D	-	$3 \times 3$	-	24	2
$192^2 \times 24$	FusedIB	-	$3 \times 3$	96	48	2
$96^2 \times 48$	ExtraDW	$3 \times 3$	$5 \times 5$	192	96	2
$48^2 \times 96$	ExtraDW	$3 \times 3$	$3 \times 3$	384	96	1
$48^2 \times 96$	ExtraDW	$3 \times 3$	$5 \times 5$	384	192	2
$24^2 \times 192$	ExtraDW	$3 \times 3$	$3 \times 3$	768	192	1
$24^2 \times 192$	ExtraDW	$3 \times 3$	$3 \times 3$	768	192	1
$24^2 \times 192$	ExtraDW	$3 \times 3$	$3 \times 3$	768	192	1
$24^2 \times 192$	ExtraDW	$3 \times 3$	$5 \times 5$	768	192	1
$24^2 \times 192$	ExtraDW	$5 \times 5$	$3 \times 3$	768	192	1
$24^2 \times 192$	ExtraDW	$5 \times 5$	$3 \times 3$	768	192	1
$24^2 \times 192$	ExtraDW	$5 \times 5$	$3 \times 3$	768	192	1
$24^2 \times 192$	ExtraDW	$5 \times 5$	$3 \times 3$	768	192	1
$24^2 \times 192$	ConvNext	$3 \times 3$	-	768	192	1
$24^2 \times 192$	ExtraDW	$5 \times 5$	$5 \times 5$	768	512	2
$12^2 \times 512$	ExtraDW	$5 \times 5$	$5 \times 5$	2048	512	1
$12^2 \times 512$	ExtraDW	$5 \times 5$	$5 \times 5$	2048	512	1
$12^2 \times 512$	ExtraDW	$5 \times 5$	$5 \times 5$	2048	512	1
$12^2 \times 512$	ConvNext	$5 \times 5$	-	2048	512	1
$12^2 \times 512$	ExtraDW	$5 \times 5$	$3 \times 3$	2048	512	1
$12^2 \times 512$	ConvNext	$5 \times 5$	-	2048	512	1
$12^2 \times 512$	ConvNext	$5 \times 5$	-	2048	512	1
$12^2 \times 512$	ExtraDW	$5 \times 5$	$3 \times 3$	2048	512	1
$12^2 \times 512$	ExtraDW	$5 \times 5$	$5 \times 5$	2048	512	1
$12^2 \times 512$	ConvNext	$5 \times 5$	-	2048	512	1
$12^2 \times 512$	ConvNext	$5 \times 5$	-	2048	512	1
$12^2 \times 512$	ConvNext	$5 \times 5$	-	2048	512	1
$12^2 \times 512$	Conv2D	-	$1 \times 1$	-	960	1
$12^2 \times 960$	AvgPool	-	$12 \times 12$	-	960	1
$1^2 \times 960$	Conv2D	-	$1 \times 1$	-	1280	1
$1^2 \times 1280$	Conv2D	-	$1 \times 1$	-	1000	1

**Table 13:** Architecture specification of MNv4-Conv-L.

Input	Block	DW $K_1$	DW $K_2$	Expanded Dim	Output Dim	Stride
$384^2 \times 3$	Conv2D	-	$3 \times 3$	-	24	2
$192^2 \times 24$	FusedIB	-	$3 \times 3$	96	48	2
$96^2 \times 48$	ExtraDW	$3 \times 3$	$5 \times 5$	192	96	2
$48^2 \times 96$	ExtraDW	$3 \times 3$	$3 \times 3$	384	96	1
$48^2 \times 96$	ExtraDW	$3 \times 3$	$5 \times 5$	384	192	2
$24^2 \times 192$	ExtraDW	$3 \times 3$	$3 \times 3$	768	192	1
$24^2 \times 192$	ExtraDW	$3 \times 3$	$3 \times 3$	768	192	1
$24^2 \times 192$	ExtraDW	$3 \times 3$	$3 \times 3$	768	192	1
$24^2 \times 192$	ExtraDW	$3 \times 3$	$5 \times 5$	768	192	1
$24^2 \times 192$	ExtraDW	$5 \times 5$	$3 \times 3$	768	192	1
$24^2 \times 192$	ExtraDW	$5 \times 5$	$3 \times 3$	768	192	1
$24^2 \times 192$	Mobile-MQA	-	-	-	192	1
$24^2 \times 192$	ExtraDW	$5 \times 5$	$3 \times 3$	768	192	1
$24^2 \times 192$	Mobile-MQA	-	-	-	192	1
$24^2 \times 192$	ExtraDW	$5 \times 5$	$3 \times 3$	768	192	1
$24^2 \times 192$	Mobile-MQA	-	-	-	192	1
$24^2 \times 192$	ExtraDW	$5 \times 5$	$3 \times 3$	768	192	1
$24^2 \times 192$	Mobile-MQA	-	-	-	192	1
$24^2 \times 192$	ConvNext	$3 \times 3$	-	768	192	1
$24^2 \times 192$	ExtraDW	$5 \times 5$	$5 \times 5$	768	512	2
$12^2 \times 512$	ExtraDW	$5 \times 5$	$5 \times 5$	2048	512	1
$12^2 \times 512$	ExtraDW	$5 \times 5$	$5 \times 5$	2048	512	1
$12^2 \times 512$	ExtraDW	$5 \times 5$	$5 \times 5$	2048	512	1
$12^2 \times 512$	ConvNext	$5 \times 5$	-	2048	512	1
$12^2 \times 512$	ExtraDW	$5 \times 5$	$3 \times 3$	2048	512	1
$12^2 \times 512$	ConvNext	$5 \times 5$	-	2048	512	1
$12^2 \times 512$	ConvNext	$5 \times 5$	-	2048	512	1
$12^2 \times 512$	ExtraDW	$5 \times 5$	$3 \times 3$	2048	512	1
$12^2 \times 512$	ExtraDW	$5 \times 5$	$5 \times 5$	2048	512	1
$12^2 \times 512$	Mobile-MQA	-	-	-	512	1
$12^2 \times 512$	ConvNext	$5 \times 5$	-	2048	512	1
$12^2 \times 512$	Mobile-MQA	-	-	-	512	1
$12^2 \times 512$	ConvNext	$5 \times 5$	-	2048	512	1
$12^2 \times 512$	Mobile-MQA	-	-	-	512	1
$12^2 \times 512$	ConvNext	$5 \times 5$	-	2048	512	1
$12^2 \times 512$	Mobile-MQA	-	-	-	512	1
$12^2 \times 512$	ConvNext	$5 \times 5$	-	2048	512	1
$12^2 \times 512$	Conv2D	-	$1 \times 1$	-	960	1
$12^2 \times 960$	AvgPool	-	$12 \times 12$	-	960	1
$1^2 \times 960$	Conv2D	-	$1 \times 1$	-	1280	1
$1^2 \times 1280$	Conv2D	-	$1 \times 1$	-	1000	1

Table 14: Architecture specification of MNv4-Hybrid-L.

### E Larger Pareto curve

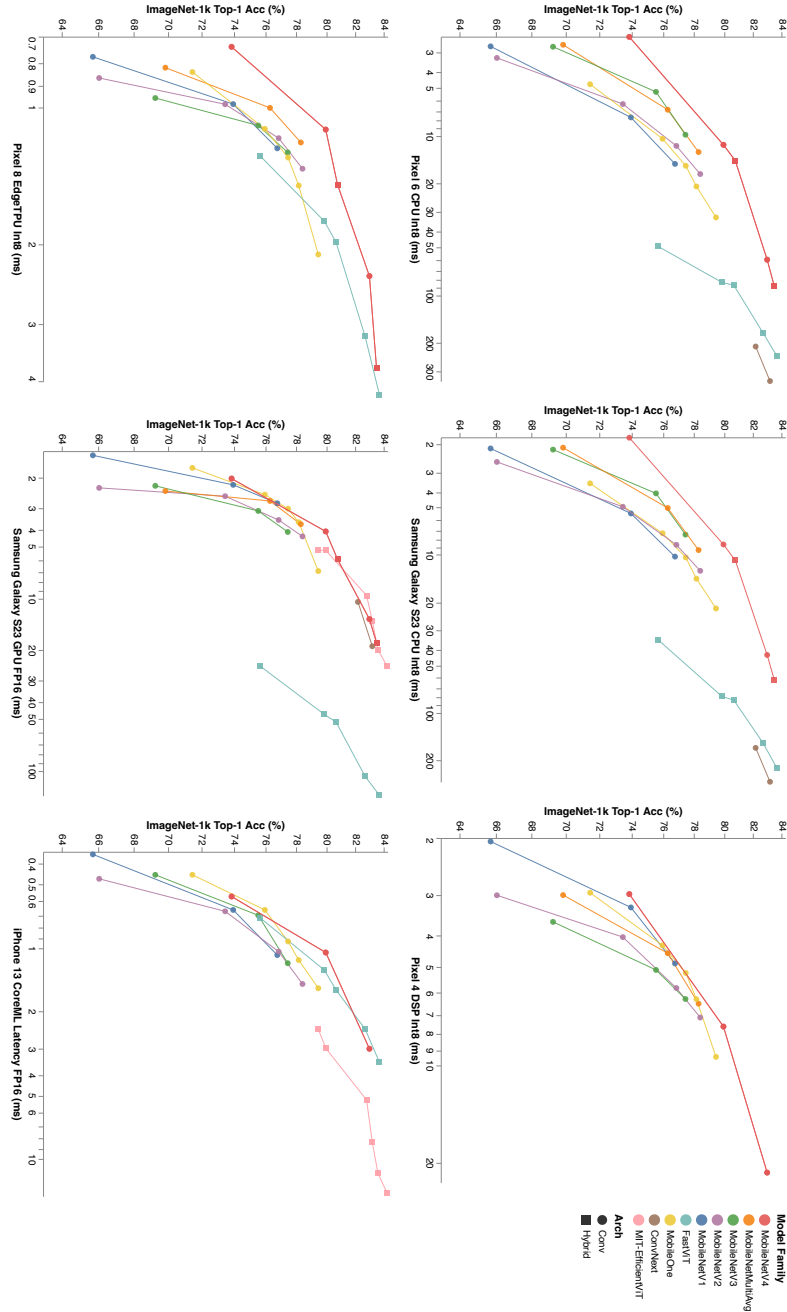


**Fig. 5: MNv4 Models are Universally Mostly Pareto Optimal:** This is the same chart as Fig. 1, but expanded to be easier to read.

## F Additional Roofline Analysis

This extends the analysis from Fig. 3 to include MobileNetV4-Conv-Small (Fig. 7), MobileNetV4-Conv-Medium (Fig. 8), and MobileNetV4-Conv-Large (Fig. 9). These figures also break out each order of magnitude in the sweep from a 0.0 MACs/byte ridge point (MACs-only, infinite memory bandwidth) to a 500.0 MACs/byte ridge point (Accelerator-like, bottlenecked on memory bandwidth). Also included is a correlation analysis between measured latencies, empirically-fit roofline models, and counting MACs (Table 15 and Fig. 6).

Execution Target	Ridge Point (MACs/B)	$r_s$ -Roofline	$r_s$ -MAC
Pixel 6 CPU (Int8)	31.2	0.973	0.962
Samsung Galaxy S23 CPU (Int8)	39.7	0.962	0.940
Pixel 4 DSP (Int8)	347.3	0.962	0.758
Pixel 8 EdgeTPU (Int8)	433.8	0.973	0.857

**Table 15: Correlation Between Roofline Models and Real Hardware:** The Ridge Points (RPs) for these roofline models were empirically fit to the networks’ measured performance.  $r_s$ -Roofline is Spearman’s rank correlation coefficient between the target’s measured latencies and roofline predictions.  $r_s$ -MAC is rank correlation between the target’s measured latencies and the networks’ MAC counts. Counting MACs has high rank correlation for low-RP targets, but much lower rank correlation for high-RP targets.  $r_s$ -Roofline is high for all targets under consideration. This shows the accuracy improvement from considering memory bandwidth in addition to MACs when estimating latency. All Ridge Point (RP) values fit in the 0-500 MACs/B range considered in our design analysis. These results are visualized in Fig. 6.

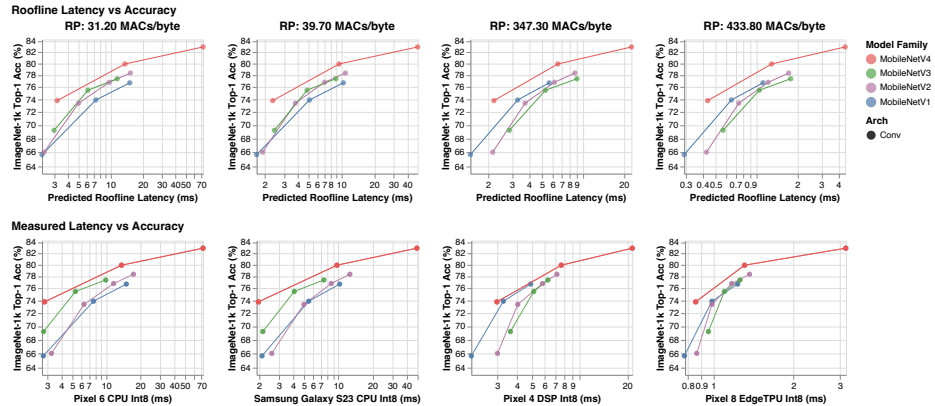


**Fig. 6: Correlation Between Roofline Models and Real Hardware:** These are the models considered in Table 15. The roofline models successfully capture the relative ordering of each model family on each hardware target with respect to the Pareto frontier, but there is additional nuance on each target that is not captured by the roofline models.

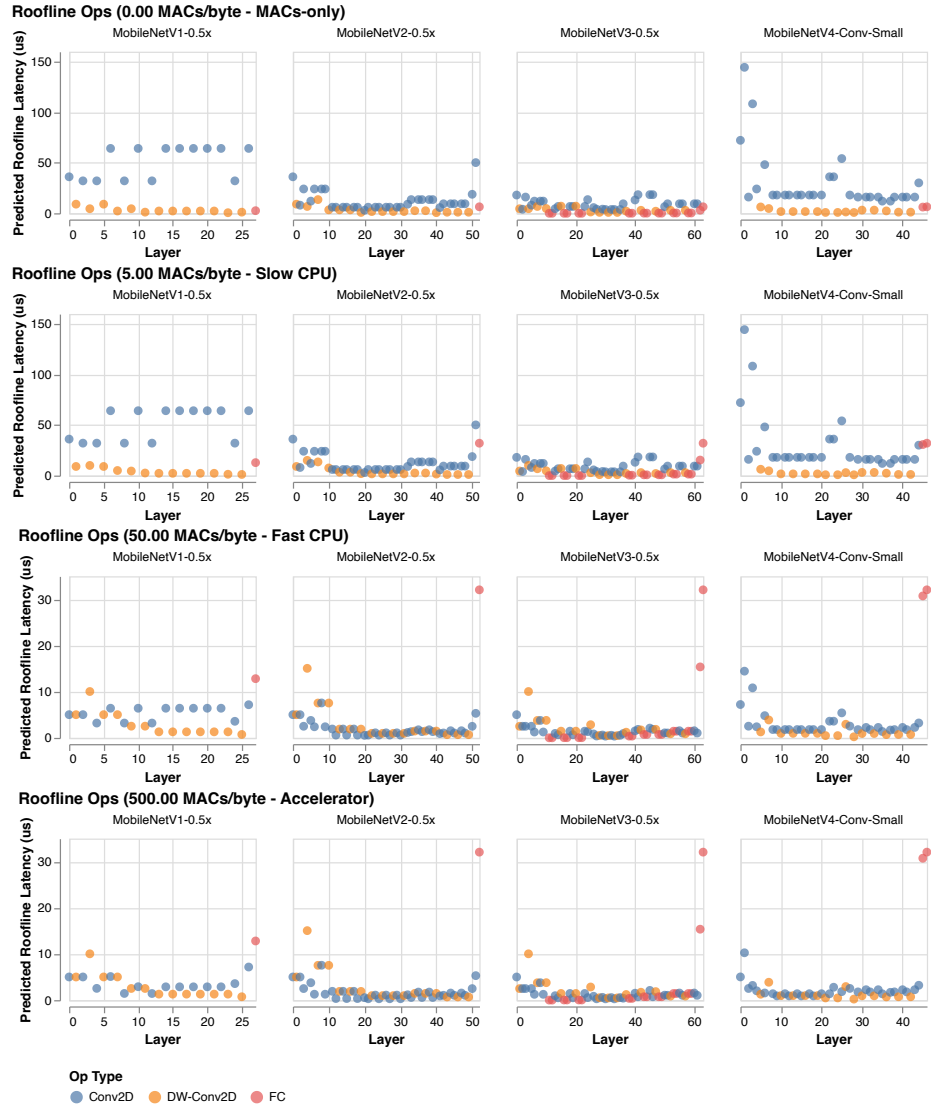


Fig. 7: Roofline RP Sweep Analysis - Small Models

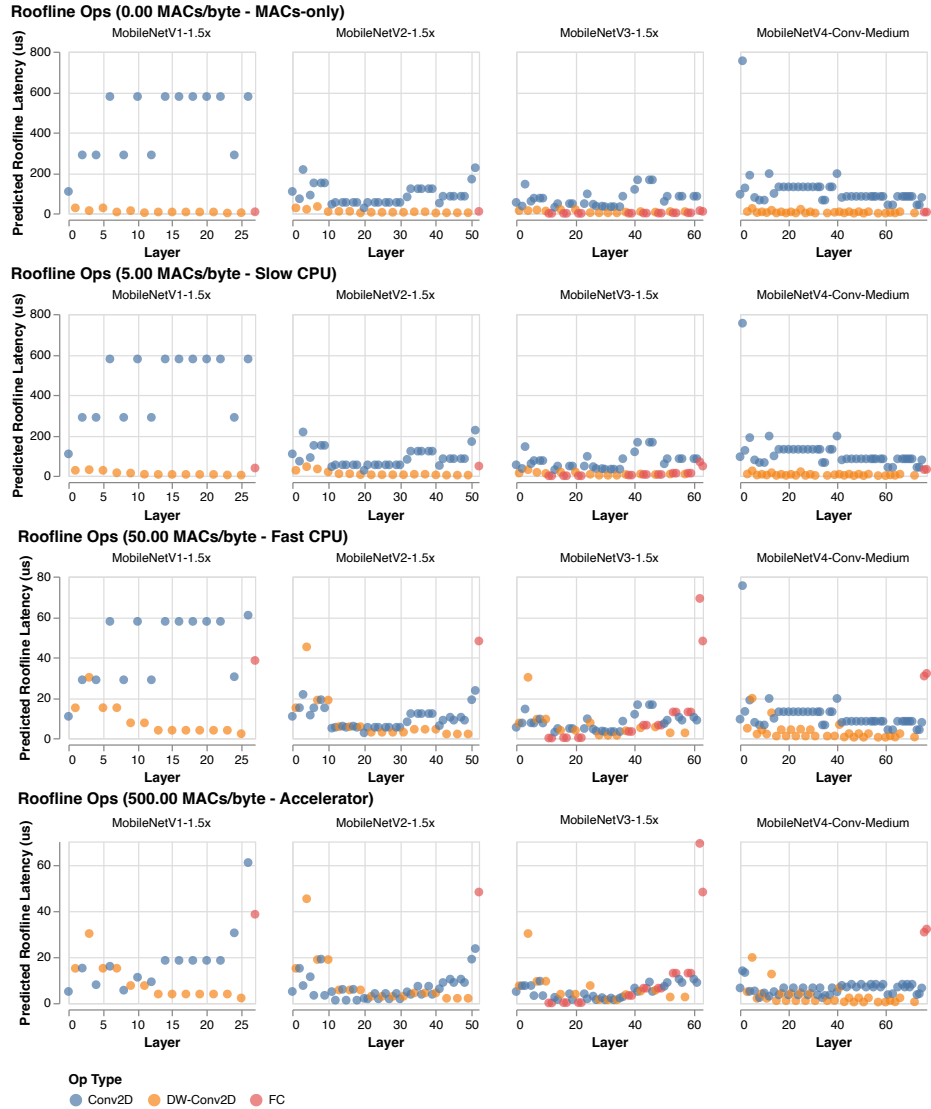
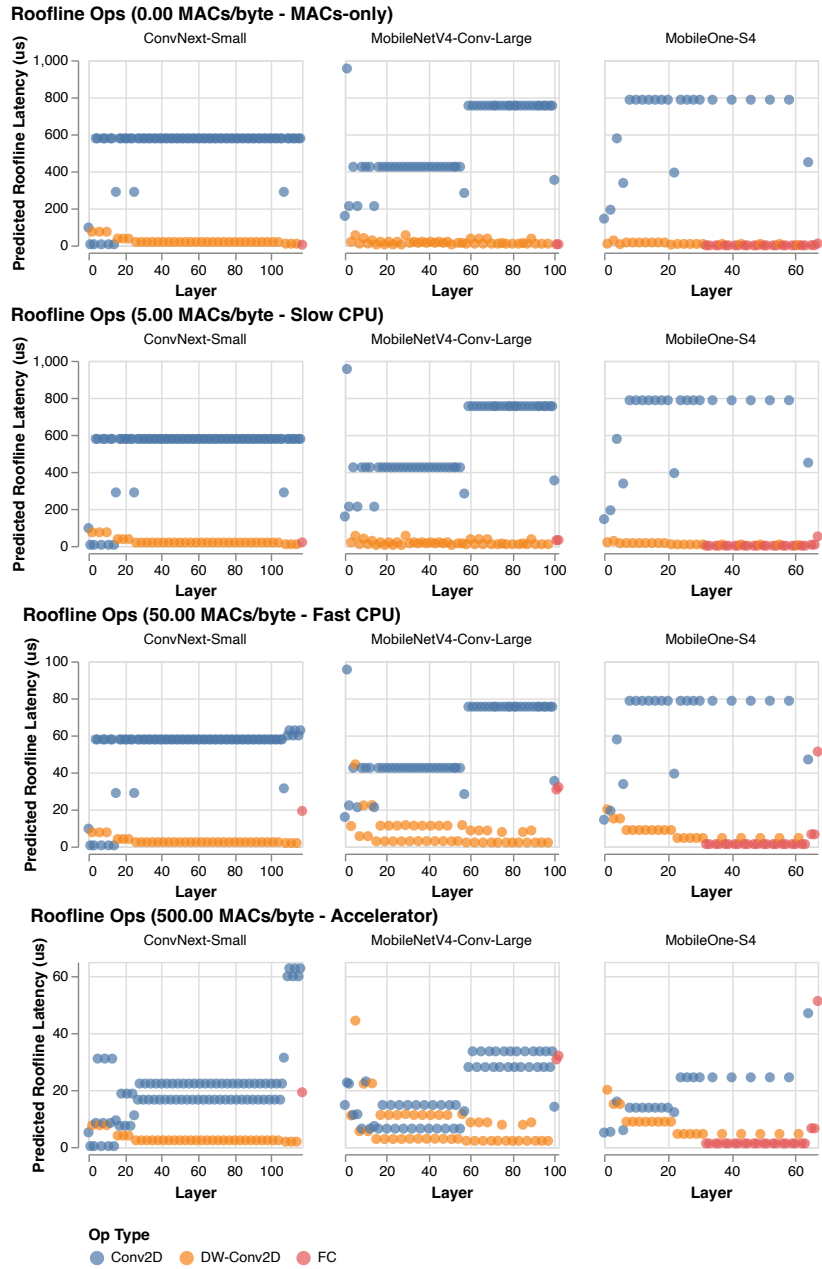


Fig. 8: Roofline RP Sweep Analysis - Medium Models



**Fig. 9: Roofline RP Sweep Analysis - Large Models:** No previous convolutional MobileNets are as big as MobileNetV4-Conv-Large, so this compares to ConvNext-Small and MobileOne-S4 for contrast. ConvNext-Small is included because it has a similar latency to MobileNetV4-Conv-Large on S23 GPU. MobileOne-S4 is included because it has a similar latency to MobileNetV4-Conv-Large on Pixel 8 EdgeTPU.